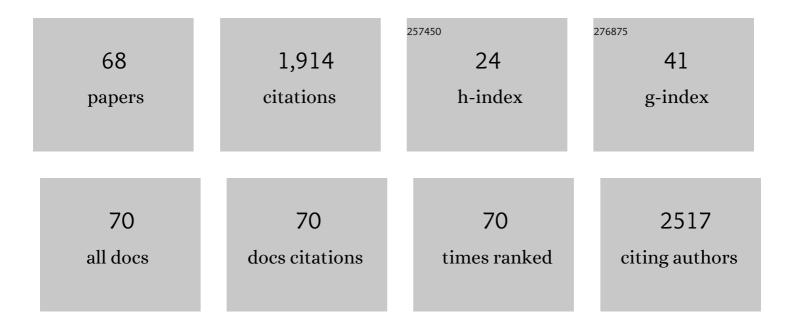
List of Publications by Year in descending order

Source: https://exaly.com/author-pdf/7271912/publications.pdf Version: 2024-02-01



Іліс 7ноц

#	Article	IF	CITATIONS
1	Controllable sites and high-capacity immobilization of uranium in Nd ₂ Zr ₂ O ₇ pyrochlore. Journal of Synchrotron Radiation, 2022, 29, 37-44.	2.4	8
2	Dynamic structural transformation induced by defects in nano-rod FeOOH during electrochemical water splitting. Journal of Materials Chemistry A, 2022, 10, 602-610.	10.3	18
3	Recovery of a generic local Hamiltonian from a steady state. Physical Review A, 2022, 105, .	2.5	3
4	Atomic controllable anchoring of uranium into zirconate pyrochlore with ultrahigh loading capacity. Chemical Communications, 2022, 58, 3469-3472.	4.1	3
5	<i>In Situ</i> Exploring of the Origin of the Enhanced Oxygen Evolution Reaction Efficiency of Metal(Co/Fe)–Organic Framework Catalysts Via Postprocessing. ACS Catalysis, 2022, 12, 3138-3148.	11.2	24
6	5f Covalency Synergistically Boosting Oxygen Evolution of UCoO ₄ Catalyst. Journal of the American Chemical Society, 2022, 144, 416-423.	13.7	48
7	Nonmonotonic wavelength dependence of the polarization-sensitive infrared photoresponse of an anisotropic semimetal. Nanoscale, 2022, 14, 7314-7321.	5.6	1
8	Enhanced photodetector performance of black phosphorus by interfacing with chiral perovskite. Nano Research, 2022, 15, 7492-7497.	10.4	12
9	Growth of LaCoO ₃ crystals in molten salt: effects of synthesis conditions. CrystEngComm, 2021, 23, 671-677.	2.6	5
10	Combined role of polarization matching and critical coupling in enhanced absorption of 2D materials based on metamaterials. Optics Express, 2021, 29, 9269.	3.4	13
11	Dynamically tunable ultra-narrowband perfect absorbers for the visible-to-infrared range based on a microcavity integrated graphene pair. Optics Letters, 2021, 46, 2236.	3.3	10
12	Nonlocal effective-medium theory for periodic multilayered metamaterials. Journal of Optics (United) Tj ETQq0 0	0 rgBT /O	verlock 10 Tf
13	Tailored Brownmillerite Oxide Catalyst with Multiple Electronic Functionalities Enables Ultrafast Water Oxidation. Chemistry of Materials, 2021, 33, 5233-5241.	6.7	32
14	Enhancing Thermocatalytic Activities by Upshifting the dâ€Band Center of Exsolved Coâ€Niâ€Fe Ternary Alloy Nanoparticles for the Dry Reforming of Methane. Angewandte Chemie, 2021, 133, 16048-16055.	2.0	11
15	Enhancing Thermocatalytic Activities by Upshifting the dâ€Band Center of Exsolved Coâ€Niâ€Fe Ternary Alloy Nanoparticles for the Dry Reforming of Methane. Angewandte Chemie - International Edition, 2021, 60, 15912-15919.	13.8	65
16	Carbon Nanotube Far Infrared Detectors with High Responsivity and Superior Polarization Selectivity Based on Engineered Optical Antennas. Sensors, 2021, 21, 5221.	3.8	2

17	Integrated Photonic Structure Enhanced Infrared Photodetectors. Advanced Photonics Research, 2021, 2, 2000187.	3.6
----	----------------------------------------------------------------------------------------------------------------	-----

18Quantum well infrared detectors enhanced by faceted plasmonic cavities. Infrared Physics and
Technology, 2021, 116, 103746.2.912

#	Article	IF	CITATIONS
19	In Situ/Operando Capturing Unusual Ir ⁶⁺ Facilitating Ultrafast Electrocatalytic Water Oxidation. Advanced Functional Materials, 2021, 31, 2104746.	14.9	29
20	A Tunable Amorphous Heteronuclear Iron and Cobalt Imidazolate Framework Analogue for Efficient Oxygen Evolution Reactions. European Journal of Inorganic Chemistry, 2021, 2021, 702-707.	2.0	7
21	Metamaterial integrated circular polarization quantum well infrared photodetectors. , 2021, , .		0
22	Cavity coupled plasmonic resonator enhanced infrared detectors. Applied Physics Letters, 2021, 119, .	3.3	6
23	<i>A</i> '– <i>B</i> Intersite Cooperation-Enhanced Water Splitting in Quadruple Perovskite Oxide CaCu ₃ Ir ₄ O ₁₂ . Chemistry of Materials, 2021, 33, 9295-9305.	6.7	11
24	First-Principles Insight into the Effects of Intrinsic Oxygen Defects on Proton Conduction in Ruddlesden–Popper Oxides. Journal of Physical Chemistry Letters, 2021, 12, 11503-11510.	4.6	7
25	Narrowband tunable graphene perfect absorber based on dielectric microcavity in mid-infrared. , 2021, , .		0
26	Metamaterial optical antennas powered carbon nanotube detectors with extremely high polarization selectivity. , 2021, , .		0
27	A Dualâ€Gate MoS ₂ Photodetector Based on Interface Coupling Effect. Small, 2020, 16, e1904369.	10.0	65
28	Enhanced infrared photoresponse induced by symmetry breaking in a hybrid structure of graphene and plasmonic nanocavities. Carbon, 2020, 170, 49-58.	10.3	15
29	Molten Salt Treated Cu Foam Catalyst for Selective Electrochemical CO 2 Reduction Reaction. ChemistrySelect, 2020, 5, 11927-11933.	1.5	6
30	Modulated synthesis and isoreticular expansion of Th-MOFs with record high pore volume and surface area for iodine adsorption. Chemical Communications, 2020, 56, 6715-6718.	4.1	81
31	Identifying the electrocatalytic active sites of a Ru-based catalyst with high Faraday efficiency in CO ₂ -saturated media for an aqueous Zn–CO ₂ system. Journal of Materials Chemistry A, 2020, 8, 14927-14934.	10.3	16
32	Tuning Electrical and Optical Properties of MoSe ₂ Transistors via Elemental Doping. Advanced Materials Technologies, 2020, 5, 2000307.	5.8	15
33	Enhancing Bifunctional Electrocatalytic Activities via Metal d-Band Center Lift Induced by Oxygen Vacancy on the Subsurface of Perovskites. ACS Catalysis, 2020, 10, 4664-4670.	11.2	116
34	Highly polarization-sensitive far infrared detector based on an optical antenna integrated aligned carbon nanotube film. Nanoscale, 2020, 12, 11808-11817.	5.6	12
35	Circular Polarization Discrimination Enhanced by Anisotropic Media. Advanced Optical Materials, 2020, 8, 1901800.	7.3	20
36	Voltage- and time-dependent valence state transition in cobalt oxide catalysts during the oxygen evolution reaction. Nature Communications, 2020, 11, 1984.	12.8	120

#	Article	IF	CITATIONS
37	HgCdTe mid-Infrared photo response enhanced by monolithically integrated meta-lenses. Scientific Reports, 2020, 10, 6372.	3.3	23
38	Absorption enhancement in all-semiconductor plasmonic cavity integrated THz quantum well infrared photodetectors. Optics Express, 2020, 28, 16427.	3.4	13
39	Investigation of the local structure of molten ThF ₄ –LiF and ThF ₄ –LiF–BeF ₂ mixtures by high-temperature X-ray absorption spectroscopy and molecular-dynamics simulation. Journal of Synchrotron Radiation, 2019, 26, 1733-1741.	2.4	11
40	Enhanced polarization sensitivity by plasmonic-cavity in graphene phototransistors. Journal of Applied Physics, 2019, 126, .	2.5	19
41	Realization of Both High Absorption of Active Materials and Low Ohmic Loss in Plasmonic Cavities. Advanced Optical Materials, 2019, 7, 1801627.	7.3	23
42	Cut-off wavelength manipulation of pixel-level plasmonic microcavity for long wavelength infrared detection. Applied Physics Letters, 2019, 114, .	3.3	6
43	Large-area, lithography-free, narrow-band and highly directional thermal emitter. Nanoscale, 2019, 11, 19742-19750.	5.6	39
44	Top-gated black phosphorus phototransistor for sensitive broadband detection. Nanoscale, 2018, 10, 5852-5858.	5.6	19
45	High extinction ratio super pixel for long wavelength infrared polarization imaging detection based on plasmonic microcavity quantum well infrared photodetectors. Scientific Reports, 2018, 8, 15070.	3.3	29
46	Reconstructing a plasmonic metasurface for a broadband high-efficiency optical vortex in the visible frequency. Nanoscale, 2018, 10, 12378-12385.	5.6	13
47	All-dielectric resonant waveguide based quantum well infrared photodetectors for hyperspectral detection. Optics Communications, 2018, 427, 196-201.	2.1	16
48	Visualizing Mie Resonances in Low-Index Dielectric Nanoparticles. Physical Review Letters, 2018, 120, 253902.	7.8	28
49	Toward Sensitive Room‶emperature Broadband Detection from Infrared to Terahertz with Antennaâ€Integrated Black Phosphorus Photoconductor. Advanced Functional Materials, 2017, 27, 1604414.	14.9	88
50	Engineering Light at the Nanoscale: Structural Color Filters and Broadband Perfect Absorbers. Advanced Optical Materials, 2017, 5, 1700368.	7.3	141
51	Wavelength scale terahertz spectrometer based on extraordinary transmission. Applied Physics Letters, 2017, 111, 063503.	3.3	2
52	Semitransparent and Flexible Mechanically Reconfigurable Electrically Small Antennas Based on Tortuous Metallic Micromesh. IEEE Transactions on Antennas and Propagation, 2017, 65, 150-158.	5.1	58
53	Efficient Thermal–Light Interconversions Based on Optical Topological Transition in the Metalâ€Dielectric Multilayered Metamaterials . Advanced Materials, 2016, 28, 3017-3023.	21.0	38
54	Large-Area High Aspect Ratio Plasmonic Interference Lithography Utilizing a Single High- <i>k</i> Mode. ACS Nano, 2016, 10, 4039-4045.	14.6	58

#	Article	IF	CITATIONS
55	Angle Robust Reflection/Transmission Plasmonic Filters Using Ultrathin Metal Patch Array. Advanced Optical Materials, 2016, 4, 1981-1986.	7.3	44
56	Light Coupling Engineering of a Double-Pinhole Nanoresonator. Journal of Nanoscience and Nanotechnology, 2016, 16, 8130-8134.	0.9	0
57	White light emission and optical gains from a Si nanocrystal thin film. Nanotechnology, 2015, 26, 475203.	2.6	24
58	Transparent and mechanically reconfigurable small antenna based on stretchable micromesh. , 2015, , .		1
59	Experiment and Theory of the Broadband Absorption by a Tapered Hyperbolic Metamaterial Array. ACS Photonics, 2014, 1, 618-624.	6.6	208
60	Transition from a spectrum filter to a polarizer in a metallic nano-slit array. Scientific Reports, 2014, 4, 3614.	3.3	35
61	Transition from a color filter to a polarizer of a metallic nano-slit array. , 2013, , .		2
62	A close to unity and all-solar-spectrum absorption by ion-sputtering induced Si nanocone arrays. Optics Express, 2012, 20, 22087.	3.4	25
63	Nanopatterning of Si surfaces by normal incident ion erosion: Influence of iron incorporation on surface morphology evolution. Journal of Applied Physics, 2011, 109, .	2.5	47
64	Self-organized antireflecting nano-cone arrays on Si (100) induced by ion bombardment. Journal of Applied Physics, 2011, 109, .	2.5	34
65	Mechanism of Fe impurity motivated ion-nanopatterning of Si (100) surfaces. Physical Review B, 2010, 82, .	3.2	43
66	A refined Ehrlich–Schwoebel effect on the modification of Si surface nanostructures by post ion milling. Applied Surface Science, 2008, 254, 2238-2243.	6.1	2
67	The effect of Ehrlich–Schwoebel step-edge barrier on the formation of self-organized Si nanodots by ion-sputter erosion. Applied Surface Science, 2007, 253, 4497-4500.	6.1	3
68	An electrostatic force microscope study of Si nanostructures on Si(100) as a function of post-annealing temperature and time. Applied Surface Science, 2007, 253, 6109-6112.	6.1	14